Science of the Total Environment 845 (2022) 157314

Contents lists available at ScienceDirect

Science of the Total Environment

journal homepage: www.elsevier.com/locate/scitotenv

Methodology for assessing the vulnerability of built cultural heritage

Laura Damas Mollá [a,*], Maialen Sagarna [b], Ane Zabaleta [a], Arantza Aranburu [a], Iñaki Antiguedad [a], Jesus A. Uriarte [a]

[a] Department of Geology, Faculty of Science and Technology, University of the Basque Country, Barrio Sarriena, s/n 48970, Leioa, Spain
[b] Department of Architecture, Faculty of Engineering, University of the Basque Country UPV/EHU, Plaza Europa 1, E-20018 Donostia, Spain

HIGHLIGHTS

- A method for quantifying global vulnerability in built heritage is proposed.
- The method links the disturbances present, the factors involved and vulnerability.
- Constructive, intrinsic material, natural and environmental factors are considered.
- Several indices are obtained and represented in graphical and intuitive diagrams.
- This proposal allows for comparisons of different buildings and environments.

GRAPHICAL ABSTRACT

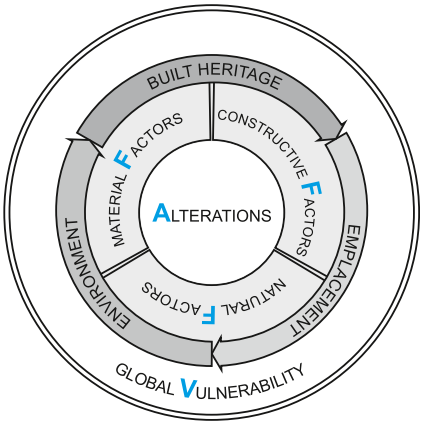

ARTICLE INFO

Editor: Philip K. Hopke

Keywords:
Diagram AFV
Alterations
Vulnerability
Constructions
Cultural heritage

ABSTRACT

The conservation of constructions, and especially of built heritage, requires complex studies concerning their Global Vulnerability. These studies have to consider the current state of the building, i.e. the degradation degree, and the factors that mostly affect the building and, therefore, generate alterations. These factors are not limited to the structure of the building, location and environmental factors are also involved. Hence, the assessment of built heritage vulnerability should consider the building itself and also be extended to the site and the environment. This work presents a systematic and reproducible methodology for the quantification of the Global Vulnerability in different typologies of constructions and environments. The proposed methodology establishes a relationship between the existing alterations (A) and the main factors (F) that affect vulnerability (V) by means of an AFV (Alteration/Factor/Vulnerability) diagram. Based on these results alteration and vulnerability indices are calculated. The obtained AFV diagram allows the comparison between different constructions or separate areas within the same construction. This methodology was validated in two early twentieth-century constructions that form part of the reinforced concrete architectural heritage of the Basque Country: the Punta Begoña Galleries (Getxo, Spain) and the Aqueduct of the Araxes paper mill (Tolosa, Spain).

1. Introduction and objectives

A diagnosis of the state of built cultural heritage is a very delicate task (Fais et al., 2018), and requires an anamnesis of different aspects, including construction factors, factors intrinsic to the building materials themselves and natural and environmental factors (Esbert et al., 1997; Alonso et al., 2006; Mateos Redondo, 2012; Moropoulou et al., 2013). These three groups of factors are the triggers of the alterations observed in constructions (International Council on Monuments and Sites (ICOMOS, 2010); Laborde Marqueze, 2013; Damas Mollá et al., 2018). Therefore, the quantification of Global Vulnerability in built heritage requires a coordinated study of

* Corresponding author.
E-mail address: laura.damas@ehu.eus (L. Damas Mollá).

http://dx.doi.org/10.1016/j.scitotenv.2022.157314
Received 7 March 2022; Received in revised form 10 June 2022; Accepted 8 July 2022
Available online 13 July 2022

alterations and factors. The assessment of the degree of Global Vulnerability of the built heritage is essential in order to subsequently determine the best specific sequence of observation (monitoring) and analysis for each case studied.

Numerous works have been published characterising the vulnerability of constructions in specific cases, many of them are based on vulnerability matrices, using specific factors that depend on different approaches (Galan and Aparicio, 2013; Ortiz and Ortiz, 2016a, 2016b; Gandini et al., 2018). Previous studies of vulnerability in architectural heritage, still in use today, focus on the weathering processes of building materials (Pope et al., 2002; Hatir, 2020). There are also numerous studies assessing vulnerability to natural hazards (Álvarez et al., 2017; Fakhruddin et al., 2019; Prasetyo et al., 2020), such as earthquakes (Formisano and Marzo, 2017; Fotopoulou and Pitilakis, 2017; Quagliarini et al., 2019) and landslides (Papathoma-Köhle et al., 2017; Bera et al., 2020; D'Ayala et al., 2020). Other studies focus on specific factors such as coastal processes (Reeder-Myers, 2015; Mattei et al., 2019; Rodriguez-Rosales et al., 2021). Some studies reflect the need to assess the interactions between different factors, constructive and natural factors, and consequent damages. Thus, the classification established in the European Macroseismic Scale 1998 (European Center for Geodynamics and Seismology, 1998) considers the type of materials in a building, their structural execution and earthquakes. Valuzzi et al. (2020) and Borri et al. (2020) addressed the correlation between alterations and vulnerability, and included the assessment of the artistic assets in the structure of the buildings. The studies related to climate change impact on built heritage are also a good example of this type of interplay analysis, as they assess the interaction between different variables (Daly, 2014; Sesana et al., 2018; Day et al., 2020; Edmonds et al., 2020; Fatorić and Biesbroek, 2020; Prieto et al., 2020; Bienvenido-Huertas et al., 2021; Bonazza et al., 2021; Cacciotti et al., 2021).

The specific nature of such studies of the vulnerability of architectural heritage makes them difficult to reproduce and does not enable establishing real comparisons of Global Vulnerability between different buildings. For that reason, it is necessary to provide a common methodology for a first vulnerability assessment that will establish the baseline to conduct a more specific assessment at later stages. To quantify the Global Vulnerability of heritage buildings, it is necessary to develop a transdisciplinary study that involves and establishes a connection between the structure and the building materials, its state of conservation, its location and the environment in which it is located (ICOMOS, 2014; Damas Mollá et al., 2019). This study should include architectural, artistic, geological, chemical, biological or environmental data, among others.

The main purpose of this study is therefore to establish and validate a systematic methodology for the quantification of Global Vulnerability in cultural built heritage. This methodology allows the comparison of Global Vulnerability of buildings in the same environment that are made with different materials, or that have different uses (civil engineering or residential) and also a comparison of the same type of buildings located in very different environments. In addition, this methodology makes it possible to establish a link between the actual state of the buildings and the processes that cause damage to them, so that the ageing of the studied types of buildings in particular locations could be forecast.

Constructions of recent architecture form part of the general cultural heritage, and as such should serve the same aims, and be subject to the same principles of conservation and enhancement as those established for architectural heritage more widely (ICOMOS, 2014). In 1991, the Council of Europe, wishing to set out guidelines for identifying significant elements of construction, studying them and establishing appropriate measures of conservation, published its "Recommendation No. R (91)13 on the Protection of the Twentieth Century Architectural Heritage". Therefore, in order to validate this methodology, we have applied it to two early twentieth century constructions that form part of the reinforced concrete architectural heritage of the Basque Country.

2. Methodology: alteration/factors/vulnerability diagram (AFV diagram)

The proposed methodology is based on a diagram that relates the Alterations (A) affecting each construction to the main Factors influencing its degradation (F). These are used to quantify its global Vulnerability (V). Using this methodology, it is also possible to compare different constructions, or separate areas within the same building.

There are four main steps involved in creating the diagram (Fig. 1): 1) Alteration (A): at this stage, all alterations are characterised and differentiated according to the five main categories (A, B, C, D and E) established in the alteration matrix of Damas Mollá et al. (2018). A visual estimation is also made of the degree of alteration, based on the percentage of the area of the structure of the construction affected (ASA, Area of Structure Affected) by the alteration. Finally, 5 Alteration Indices are calculated, one for each type of main alteration. The quantification of the Alteration Indices is new to this work; 2) Factor (F): in this second stage, we weight the factors involved in causing alterations to the constructions and that actively condition their vulnerability. These are grouped into three main types: construction factors ($_C$), directly related to the construction and its emplacement; factors intrinsic to the materials ($_M$), related both to the construction and to the environment; and natural and environmental factors ($_N$), related to the emplacement and environment. The methodology proposed in this work assigns a series of numerical values to the different factors, based on certain established cases (Table I); 3) Vulnerability (V): in this stage, vulnerability indexes (FVI) are calculated based on the main factors involved (Construction Factor Vulnerability Index: F_CVI; Material Factor Vulnerability Index: F_MVI; and Natural Factor Vulnerability Index: F_NVI) using the data obtained in the previous stage, exported to the vulnerability matrix proposed in this work. These FVIs are also used to calculate the Global Vulnerability Index (V_GI). 4) The results obtained in each of the steps above are represented in the Alteration/Factor/Vulnerability (AFV) Diagram, which consists of three distinct graphs — a pentagon (A) and two block-diagrams (F and V).

2.1. Alterations to a building: forms of deterioration

The study of alterations proposed in this work is performed using the alteration matrix of Damas Mollá et al. (2018), which is based on the definitions and criteria determined by ICOMOS (2010). In this matrix, an alphanumeric classification is made of the alterations in the constructions, which are initially subdivided into five main categories. Each of these categories is represented by a specific colour: Type A alterations (red): cracks and deformations; Type B alterations (blue): mechanical damage and detachment; Type C alterations (green): chromatic alteration; Type D alterations (orange): deposits; type E alterations (purple): bioalterations. These main categories are divided into sub-categories, which are sequentially coded with numbers and letters. This matrix allows for greater agility when collecting field data. This methodology includes a new indicator – the alteration index – quantified from the degree of alteration obtained for each main category of alteration. This degree is calculated by the proportion of the Area of the Structure of the construction Affected by the alteration (ASA) expressed in %. The degree of alterations is expressed by a five-circle symbology. The number of black circles is established according to the following ratio:

○○○○○: no ASA; ●○○○○: < 10 % ASA; ●●○○○: 10 % to 25 % of ASA; ●●●○○: 25 % to 50 % of ASA; ●●●●○: 50 % to 75 % of ASA; ●●●●●: all ASA.

Five alteration indexes have been defined, one for each type of alteration: AI for Type A alterations; BI for Type B alterations; CI for Type C alterations; DI for Type D alterations; and EI for Type E alterations (Fig. 1). The alteration indexes are calculated using formula (1), by dividing the total degree for each

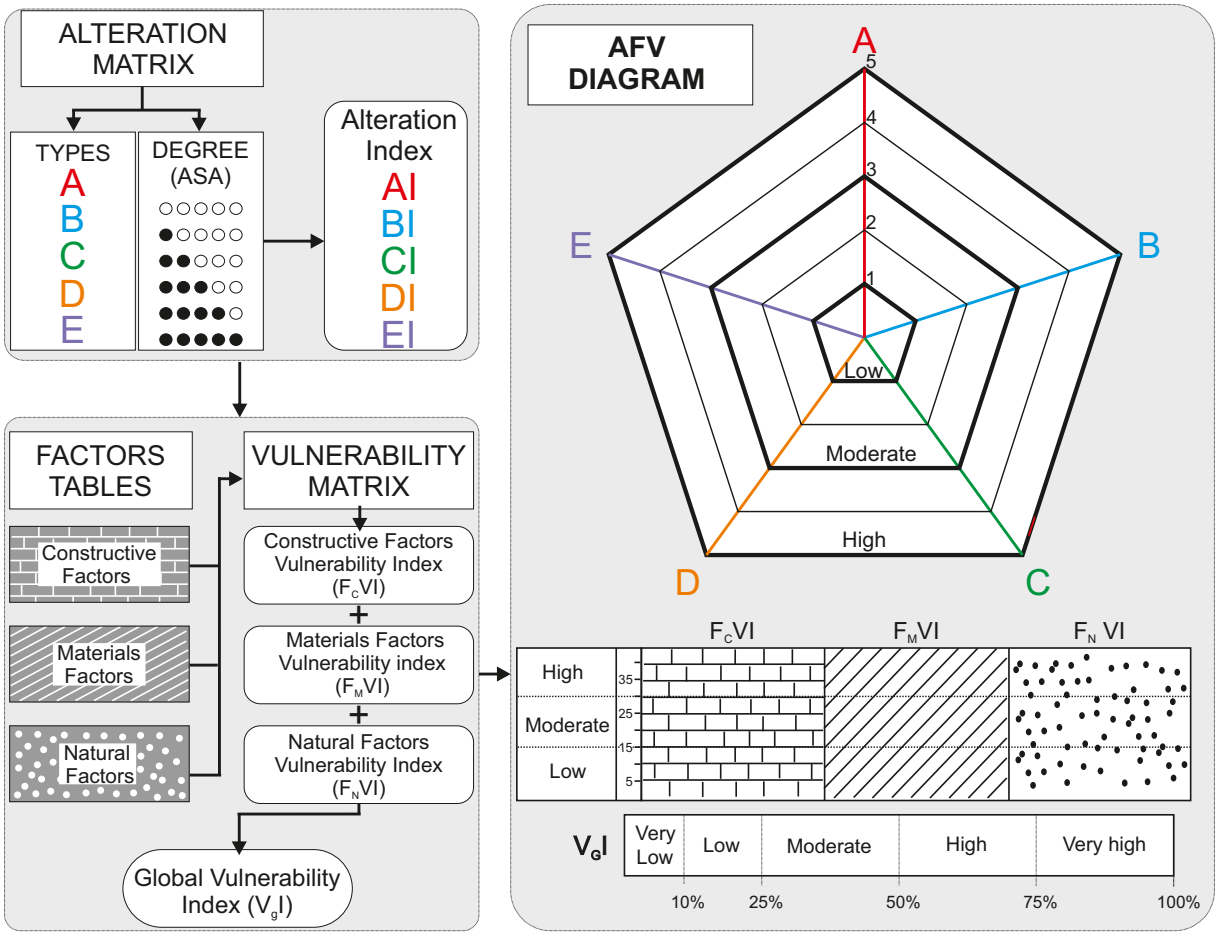

Fig. 1. Diagram of the methodology for preparing the Alteration/Factor/Vulnerability (AFV) Diagram (A, B, C, D, E: Types of alteration, as per Damas Mollá et al., 2018).

type of main alteration (sum of the scores, black circles) by the record of alterations of that type ($\mathbf{n}_{alt}$) in the construction.

$$\text{Alteration}_{(\text{A or B or C or D or E})}\text{Index} = \sum \frac{\text{total degree}_{(\text{A or B or C or D or E})}}{\mathbf{n}_{alt(\text{A or B or C or D or E})}} \quad (1)$$

For example, 3 records of type B alterations have been registered in a construction and a degree of 1 score has been obtained for the first one, 3 for the second one and 3 for the third one. The BI, obtained in this case, is 2.33 and has been obtained by dividing the sum of the scores (7) by the sum of the records of that alteration (3). Thus, each alteration index has a maximum score of 5. It can thus be represented in the radii of the pentagon in the AFV diagram (Fig. 1). Each index is marked in the colour corresponding to the type of alteration, using the criteria previously established. All points are plotted to obtain a geometric figure inside the pentagon. There are three ranges of alteration incidence, depending on the index score: < 1 low; 1 < moderate <3; and > 3 high. In this way, a graph can be produced showing which type(s) of alteration affect the construction most intensely.

2.2. Factors of vulnerability

The referenced factors involved in the vulnerability of and alterations in the built heritage can be divided into three main groups (Fig. 1): I) Construction Factors; II) Factors Intrinsic to the Construction Materials; and III) Natural and Environmental Factors (Esbert et al., 1997; Alonso et al., 2006; Mateos Redondo, 2012). These principal groups of factors may be divided into sub-factors which, in turn, contain several different categories, all of which are shown in Table I. These sub-factors have mostly been selected from previous work on building vulnerability assessment (Galan and Aparicio, 2013; Ortiz and Ortiz, 2016a).

To weight the value of each category, Table I establishes four possible cases for each one, scored from 0 to 3. Details of the procedure for the first category are given below. The same procedure will be followed for all the other categories. Construction factors have been divided into five sub-factors which are in turn subdivided into a total of fifteen categories (Table I). For the first sub-factor (execution factors) the first category is "structure and execution". Four possible cases have been defined for this category, ranging from "correct execution according to plan", weighted as 0, to "serious mistakes in execution" weighted as 3. To evaluate this category, we identify the case that best matches the construction under study. Previous studies listing these factors as being involved in building vulnerability include Alonso et al. (2006); Broto (2006); Pope et al. (2002); Galan and Aparicio (2013); Macías-Bernal et al. (2014); Ortiz and Ortiz (2016a); Papathoma-Köhle et al. (2017); Gandini et al. (2018); D'Ayala et al. (2020); Borri et al. (2020); Prieto et al. (2020); Valuzzi et al. (2020). The orientation factor has been included because it is common that the different orientations of the facades of buildings present different alteration processes caused by the differential incidence of other factors on them, for example, the wind. The scales for elevation above sea level and the height ranges are based on the Spanish Technical Building Code (Código Técnico de la Edificación, CTE) of the Spanish Ministry of Public Works (CTE, 2022). This document defines several climatic zones according to the altitude above sea level and also sets the height limit for buildings according to wind zones. The different angles of the rainfall inclination have been selected from Broto (2006). Finally, maintenance refers to the total construction.

In the case of the factors intrinsic to the materials, four sub-factors are considered, divided into fourteen categories (Table I). Previous studies establishing the involvement of these factors in the vulnerability of constructions include Alonso et al. (1998); European Center for Geodynamics and Seismology (1998); Alonso et al. (2006); Galan and Aparicio (2013); Ortiz and Ortiz (2016a); Papathoma-Köhle et al. (2017); Prieto et al. (2020). The compressive strength ranges have been adapted to those defined by CTE (2022). For quick calculation in constructions, measurements can be carried out using the Schmidt hammer. The estimation of the categories of hardness, thermal expansion and water modifications depends on the type of construction material. In terms of hardness, it is necessary to establish whether it is abrasion or scratching, among others. For example, among natural stones quartzite is the most resistant to abrasion and scratching as quartz is the main mineral (Sánchez-Delgado et al., 2016). As regards thermal changes, each material has a characteristic coefficient of thermal expansion (α). For example, while α varies between 8 and $12{\cdot}10^{-6}$ °C^{-1} for concrete (ASM International, 2002), that of oak is $54^{6}{\cdot}10^{-6}$ °C^{-1}, this variability among materials makes it necessary to estimate values qualitatively. The same applies in the case of changes due to water, depending on the material, it is necessary to differentiate between absorption and desorption and to take into account aspects such as capillarity. For these studies, the use of Thermographic cameras and hygrometers is appropriate, as they are non-destructive techniques (NDT).

Natural and environmental factors are listed in Table I. These are divided into five sub-factors, with fifteen categories. Previous studies listing these factors as being involved in the vulnerability of constructions include: Galan and Aparicio (2013); Ortiz and Ortiz (2016a); Papathoma-Köhle

Table I
Construction factors, factors intrinsic to materials and environmental and natural factors (sub-factors and categories) affecting the vulnerability of constructions: cases and values.

	SUBFACTORS	CATEGORIES	CASES	VALUE
CONSTRUCTION FACTORS	Execution factors	Structure	Serious mistakes in execution	3
			Poor execution	2
			Correct execution, some divergence from plans	1
			Correct execution according to plan	0
		Foundations/ Roofs	Deficient foundation/roofing with progressive deterioration/third-party hazard	3
			Foundation/roofing at risk of progressive deterioration with no third-party hazard	2
			Foundation/roofing with occasional deficiencies	1
			Proper and suitable foundation/roofing	0
		Load	In general, loads are in excess of tolerated amounts	3
			Some loads are greater than tolerated	2
			Some major loads in accordance with structure	1
			Loads in accordance with structure	0
		Modifications	Heavily modified building	3
			Identifiable modifications	2
			Some occasional modifications	1
			No modifications	0
	Architectural style	Artistic value	Contains abundant artistic goods connected to structural elements	3
			Contains some artistic goods connected to structural elements	2
			Contains artistic goods separate from structural elements	1
			Does not contain associated artistic goods	0
		Ornamentation	Abundant ornaments and projections	3
			Numerous ornaments	2
			Some ornaments	1
			Minimalist style with straight lines and no ornaments	0
		Materials	> 10 different materials	3
			6–10 types of material	2
			4–5 types of material	1
			2–3 types of material	0
		Carving	Hardly any work	3
			Poorly worked in small blocks	2
			Worked in small blocks or plaques	1
			Elaborately worked in large geometric blocks or plaques	0
		Finishes	Differential between materials	3
			Irregular	2
			Polished	1
			Levelling with mechanical methods (coping)	0
	Exposure factors	Orientation	Curved exterior with numerous orientations	3
			Different perpendicular orientations	2
			Different facing orientations	1
			Same orientation	0
		Elevation	More than 600 meters abobe sea level (masl)	3
			400 - 600 masl	2
			200 - 400 masl	1
			0 - 200 masl	0
		Building Height (m)	≥ 100 m	3
			41 – 99 m	2
			16 – 40 m	1
			≤ 15 m	0
		Rain inclination	20º – 0º inclination	3
			40º – 20º inclination	2
			75º – 40º inclination	1
			90º – 75º inclination	0
	Usage factors	Uses	Free public use	3
			Controlled public use	2
			Private use with regular influx of public	1
			Private use	0
		Current situation	Abandoned	3
			Low maintenance	2
			Moderate maintenance	1
			Good maintenance	0

	SUBFACTORS	CATEGORIES	CASES	VALUES
FACTORS INTRINSIC TO THE MATERIALS	Textural factors	Binder/Matrix/Cement in natural rocks	Highly alterable	3
			Alterable	2
			Low alterability	1
			Very stable against alteration	0
		Fabric	Open and alterable fabric	3
			Non-alterable open fabric	2
			Alterable closed fabric	1
			Closed, non-alterable fabric	0
		Porosity	Abundant connected porosity	3
			Low connected porosity	2
			Abundant porosity no connected	1
			Low porosity no connected	0
	Composition factors	Mineralogy	Highly alterable and varied minerals	3
			Alterable mineralogy with little variation	2
			Varied mineralogy with little alteration	1
			Stable mineralogy with little variation	0
		Artificial component	Abundant chemistry prone to weathering	3
			Little chemistry prone to weathering	2
			Abundant chemical elements not prone to weathering	1
			No additives prone to weathering	0
	Physical Properties	Colour	Varied and easily modifiable	3
			Monochromatic and easily modifiable	2
			Varied and no modifiable	1
			Monochromatic with low variation	0
		Compressive Strength	Weak (< 5 MPa)	3
			Medium strong (5-50 MPa)	2
			Strong (50-100 MPa)	1
			Very strong (>100 MPa)	0
		Hardness	Medium	3
			Low	2
			High	1
			Very high	0
		Thermal changes	High	3
			Medium	2
			Low	1
			Very low	0
		Water modifications	Very high	3
			High	2
			Medium	1
			Low	0
	Usage factors	Structural execution	Mixed execution	3
			Irregular mansory	2
			Regular mansory or brick	1
			Continuous (Reinforced Concrete)	0
		Relationship between different materials	Incompatible materials	3
			Materials with some incompatibility	2
			Compatible materials	1
			Highly suitable materials	0
		Position in the structure	In pronounced projections, ornamental areas	3
			In very exposed areas	2
			In relatively exposed areas	1
			In protected areas	0
		Execution of artificial materials	Poorly executed	3
			Deficient execution	2
			Executed with some deficiency	1
			Well executed	0
		Maintenance	Very low maintenance	3
			Low maintenance	2
			Correct maintenance	1
			Very good maintenance	0

et al. (2017); Fakhruddin et al. (2019); Mattei et al. (2019); Prasetyo et al. (2020); Prieto et al. (2020). Data concerning internal geological factors, volcanoes and earthquakes, should be taken from official data in each country or region, for example, in Spain the National Geographical Institute data are used (IGN, 2022). The values applied to the surface water factor are those established for the flood return period as defined in the Basque Water Agency (URA) of the Basque Government for the Basque Country (URA, 2022). The fire factor considered is the environmental factor and, for its quantification, the information provided by each country or region must be accessed. In this case, the forest fire meteorological index of the Basque Country (Euskalmet, 2022) is used because it is the one that best reflects the characteristics of the sites of the buildings selected for the validation of this methodology. The meteorological data ranges applied have been selected from the data established in the Basque Meteorological Agency (Euskalmet, 2022) because it is the most suitable for the examples used for the validation of the methodology proposed in this paper. The wind value is an exception because the established data of 17 m/s is based on the Beafourt Scale of wind typologies. Finally, anthropogenic biological category refers mainly to vandalism.

2.3. Vulnerability

The vulnerability is calculated using indexes obtained by means of vulnerability matrices, as defined by Galan and Aparicio (2013) and Ortiz and Ortiz (2016a). In this case, a vulnerability matrix has been designed (Fig. 2), taking into account the three groups of factors described in the previous section. In this matrix the scores obtained in each category from the cases established in Table I are noted. The sum of the values gives the vulnerability indices for each group of factors (F_CVI: Vulnerability Index for Construction Factors; F_MVI: Vulnerability Index for Factors Intrinsic to the Materials; F_NVI: Vulnerability Index for Natural and Environmental Factors), where the maximum Vulnerability Index for the factors ($F_{(C,\ M\ or\ N\ max)}$VI) is 45 (if all categories scored the maximum of 3 in the factor table).

To represent this in the AFV diagram (Fig. 1) we use a block diagram, divided into three columns, each corresponding to one of the FVIs. Vertically, each column is divided from 0 to 45 and filled using the hatching pattern corresponding to the FVI (bricks, oblique parallel lines and dots). In addition, three intensity ranges are also considered (0–14: low intensity;

	SUBFACTORS	CATEGORIES	CASES	VALUES
NATURAL AND ENVIRONMENTAL FACTORS	Geological Factors	Substrate	Residual soil	3
			Heavily weathered rock	2
			Somewhat weathered rock	1
			Rock in sound condition or low degree of weathering	0
			High risk	3
		Internal Risks (volcanoes, earthquakes) -	Moderate risk	2
			Low risk	1
			No risk	0
	Water bodies	Underground	Permanently impacted by piezometric level	3
			Variable piezometric level, with systematic impact	2
			Variable piezometric level with occasional impact	1
			No impact from piezometric level	0
		Surface	Return period 1 year	3
			10-year return period	2
			100-year return period	1
			Out of reach of watercourse/water body	0
		Sea	Littoral environment on coastline	3
			Littoral environment not on coastline	2
			Transition environment: littoral/inland	1
			Inland non-coastal environment	0
	Pollution		Industrialised urban area	3
			Urban area	2
			Rural area	1
			Wilderness area	0
	Fire		High risk zone	3
			Medium risk zone	2
			Low risk zone	1
			Area with low-risk probability	0
	Meteorological factors	Temperature	High daily variability	3
			High seasonal variability	2
			Moderate seasonal variability	1
			Unvarying climate	0
		Precipitation	Many days with heavy rains (> 30 mm/day) throughout the year	3
			Some days with heavy rains (> 30 mm/day) throughout the year	2
			Moderate rains (<30 mm/day) throughout the year	1
			Low rains (< 250 mm/year)	0
		Wind	> 17 m/s and perpendicular to the structure	3
			> 17 m/s and parallel to the structure	2
			< 17 m/s and perpendicular to the structure	1
			< 17 m/s and parallel to the structure	0
		Humidity	Environment with annual humidity >91%	3
			Environment with annual humidity of 51-90%	2
			Environment with annual humidity of 30-50%	1
			Dry environment	0
		Sunlight	Direct exposure to sunlight > 6 hours/day	3
			Direct exposure to sunlight < 6 hours/day	2
			Oblique impact of sunlight	1
			No direct sunlight	0
	Biological factors	Anthropic damage	Non-recoverable damage	3
			Severe but recoverable damage	2
			Little damage, recoverable	1
			No damage	0
		Macro-organisms	Macro-organisms colonising the structure	3
			Macro-organisms in certain areas	2
			Isolated macro-organisms	1
			No macro-organisms surveyed	0
		Micro-organisms	Varied and abundant microorganisms	3
			Varied and occasional microorganisms	2
			Unique and abundant microorganisms	1
			Unique and occasional microorganisms	0

15–30: moderate intensity; 31–45: high intensity). By using this form of representation, it is possible to assess the vulnerability of the construction under study based on the factors described above and thus to determine which factor is most relevant to its vulnerability.

The Global Vulnerability Index (V_GI) is calculated by considering the sum of the factor indexes as a percentage of maximum possible total vulnerability, in accordance with Formula (2).

$$V_GI = \frac{F_G VI + F_M VI + F_N VI}{\sum F_{(C,M \text{ or } N \text{ max})} VI} \times 100 \quad (2)$$

i.e.

$$V_GI = \frac{F_G VI + F_M VI + F_N VI}{135} \times 100$$

Like the FVI, the V_GI (%) is represented by a block diagram (Fig. 1), in which different ranges of vulnerability are defined ($V_GI < 10$ %: very low; $10 < V_GI < 25$ %: low; $25 < V_GI < 50$ %: moderate; $50 < V_GI < 75$ %: high; $75 < V_GI$: very high), equivalent to those described by Galan and Aparicio (2013).

3. Case studies

To validate this methodology, we studied two constructions of early twentieth century reinforced concrete architectural heritage in the Basque Country (Northern Spain) (Fig. 3a): the Punta Begoña Galleries (Fig. 3b) and the Araxes Paper Mill Aqueduct (Fig. 3c). Throughout the description of the main aspects of both constructions and their comparison, the corresponding factors defined in Table I and their scores are schematically included [in square brackets].

3.1. Punta Begoña Galleries (Getxo, Spain)

The Punta Begoña Galleries (Fig. 3 b2) [Ricardo Bastida, 1918] are situated in the municipal area of Getxo (Spain), in a strategic location

VULNERABILITY MATRIX

CONSTRUCTION FACTORS

	CATEGORY	NWG	SWG	APMA
Execution Factors	Structure	1	1	1
	Foundations/Roofs	1	3	2
	Load	1	2	1
	Modifications	2	2	0
Architect. style	Artistic value	2	2	0
	Ornamentation	1	1	0
	Materials	2	2	0
	Carving	1	2	3
	Finishes	3	3	0
Expos. Factors	Guidance	3	2	0
	Elevation	0	0	0
	Building height	1	1	0
	Rain inclination	1	2	1
Usage Fact	Usage	1	1	0
	Current situation	2	2	3
	$F_{C\,Max}VI$	$F_{C\text{-}1}VI$	$F_{C\text{-}2}VI$	$F_{C\text{-}3}VI$
	45	22	26	11

MATERIAL FACTORS

	CATEGORY	NWG	SWG	APMA
Textural Factor	Binder/Matrix/Cement	2	2	2
	Fabric	0	0	0
	Porosity	2	2	1
Comp Fact	Mineralogy	1	1	2
	Chemical composition	1	1	2
Physical Factors	Colour	1	1	0
	Compressive strenght	1	1	1
	Hardness	2	2	2
	Thermal changes	2	2	0
	Water Modifications	1	1	1
Usage Factors	Structural execution	3	3	0
	Relationship other materials	1	2	0
	Position in the structure	2	2	1
	Execution artificial mat.	2	2	1
	Maintenance	3	3	3
	$F_{M\,Max}VI$	$F_{M\text{-}1}VI$	$F_{M\text{-}2}VI$	$F_{M\text{-}3}VI$
	45	24	25	16

ENVIRONMENTAL FACTORS

	CATEGORY	NWG	SWG	APMA
Geol. Fact	Substrate	0	0	0
	Volcanoes/Earthquakes	0	0	0
Water bodies	Underground	1	1	3
	Surface	0	0	3
	Sea	3	3	0
Pollution		2	2	3
Fire		0	0	1
Meteorol. Factors	Temperature	1	1	1
	Precipitation	3	3	3
	Wind	0	1	0
	Humidity	2	2	3
	Insolationn	1	2	1
Fact biol	Antropic damage	2	2	1
	Macro-organisms	2	2	2
	Micro-organisms	3	3	3
	$F_{N\,Max}VI$	$F_{N\text{-}1}VI$	$F_{N\text{-}2}VI$	$F_{N\text{-}3}VI$
	45	20	22	24

$$V_GI = (F_CVI + F_MVI + F_NVI/nF_{Max}VI) \times 100$$

V_GI	NWG	48.89%	SWG	54.07%	APMA	37.78%

Fig. 2. Vulnerability matrix applied to the two façades of the Punta Begoña Galleries (NWG: Northwest Gallery; SWG: Southwest Gallery) and the Araxes Paper Mil Aqueduct (APMA) (FVI: Vulnerability index according to the different factors; V_GI: Global Vulnerability Index).

overlooking the Cantabrian Sea at the mouth of the Nervión Estuary (*Ría de Bilbao*) [Constructive Factor; Elevation: 0; Environmental Factor; Sea: 3]. Although originally designed to fulfil the need for a retaining wall on the cliff below the Etxebarrieta family mansion [Constructive Factor; Usage factor: 1], they became emblematic of their owner's distinction and power (Damas Mollá et al., 2018). In 2001, after years of abandonment [Construction Factor, Current situation: 2, because a recovery project is underway and work has started] [Material Factor; Maintenance: 3], the Punta Begoña Galleries were catalogued as a Monumental Complex and special area of Getxo, with special qualification (Gobierno Vasco, 2001).

The exterior morphology adapts to the coastline [Material Factor; Position in the structure: 2], with two main façades running perpendicular to one another: the northwest gallery (NWG), with a winding morphology [Constructive Factor; Guidance: 3] and a height of 22 m [Constructive Factor; Built Height: 1]; and the southwest gallery (SWG), divided into two straight sections and one curved section [Constructive Factor; Guidance: 3, 2] (Fig. 3 b2). Vertically the two façades are divided into three main sections (Fig. 3 b3): a sandstone masonry base; a reinforced õconcrete section decorated with mortar quadrants; and a gallery/corridor enclosed by reinforced concrete columns and prefabricated mortar õbalusters like those protecting the roof, formed by different terraces with highly ornamented ceilings (Fig. 3 b1) [Constructive Factors; Artistic value: 2; Ornamentation: 1; Materials: 2; Carving: 1,2; Finished: 3] [Materials Factor: Structural execution: 3].

3.2. Araxes paper mill aqueduct

The Araxes Paper Mill Aqueduct (APMA) at the (Fig. 3c) was one of the first reinforced concrete constructions to be erected in Spain [José Eugenio Ribera, 1903] (Ribera, 1925; Sagarna, 2010). It forms part of the Listed Cultural Asset "Araxes Paper Mill and its hydraulic infrastructures", classed as a Monumental Complex with a medium protection status (Gobierno Vasco, 2017).

The Araxes Paper Mill is located 2 km from Tolosa (Fig. 3a), in the north-east of the Iberian Peninsula [Environmental Factor; Sea: 0]. The aqueduct was used to drive the turbines for new machinery for making fine paper (Ribera, 1902). The channel is 60 m in length and is divided into five sections with a span of 12 m each. It runs across the Araxes River and a road [Environmental Factor; water bodies surface: 3; Pollution: 3], across a 58-metre-high overpass. The straight sections are supported on 4 palisades, composed of two inclined pillars joined by braces resting on a slab, under which there is a hydraulic masonry pile reinforced with steel plates (Fig. 3 c1). The supports at either end of the channel are two abutments built with conventional reinforced concrete walls supported on the natural rock [Material Factor; structural execution: 0] (Fig. 3 c3). The upper channel case in reinforced concrete through which the water flows is a rectangle measuring 100 × 110 cm (Ribera, 1925) (Fig. 3 c2).

3.3. Comparison between the two constructions

The proposed methodology does not focus exclusively on the construction itself. The constructions selected for this study present a number of similarities and differences directly related to these factors, enabling them to be used to validate the method despite being different types of construction.

The two constructions were built in the same period (the galleries in 1917 and the aqueduct in 1903) (Sagarna, 2010). The principal construction material used is reinforced concrete, still a novelty on the Iberian Peninsula at that time (Colegio de Ingenieros de Caminos, Canales y Puertos de Madrid, 1982) [Construction Factor; Structure: 1]. However, while the aqueduct is built almost entirely in concrete [Construction Factor; Materials: 0], the galleries also include many other materials (sandstone masonry, various mortars, bricks, ornamental rocks and ceramics) (Madariaga et al., 2019) [Construction Factor; Materials: 2]. At the beginning of the twentieth century, there were no specific building regulations governing reinforced concrete, although construction was based on a number of patents which determined the way the work was executed. In the case of the galleries, architect Ricardo Bastida followed a patent by Joseph

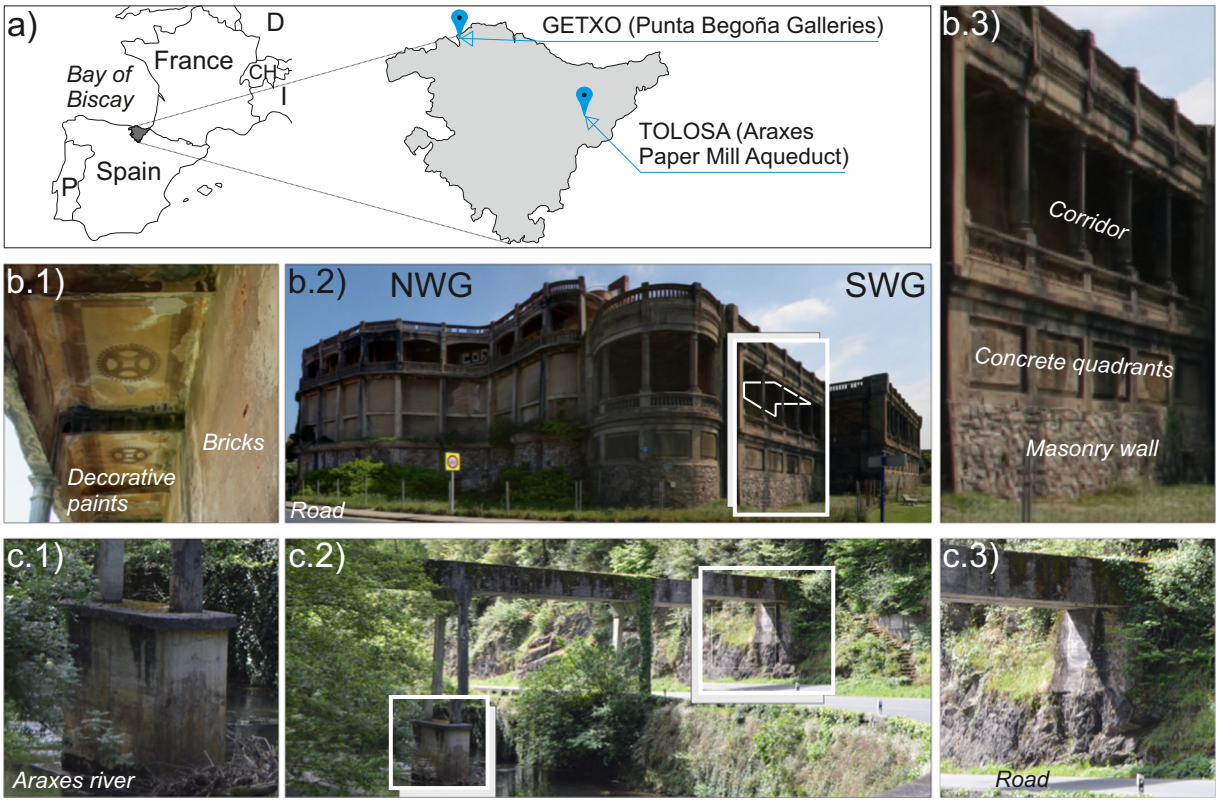

d)

	Average annual relative humidity (%)	Average annual temperature (ºC)	Annual precipitation (mm/year)	Average wind direction	Average wind speed (m/s)
Punta Begoña Galleries	89.0	14.9	967.1	SE-NW	4.97
Araxes Paper Mill Aqueduct	82.8	13.1	1565.8	NW-SE	2.47

Fig. 3. a) Geographical location of the constructions studied; b1) Ornamented ceilings in SWG of the Punta Begoña Galleries; b2) Exterior façade of the Punta Begoña Galleries (NWG: Northwest Gallery; SWG: Southwest Gallery; b3) Detail of the construction materials in the elevation of the SWG of the Punta Begoña Galleries; c1) Detail of the support of the Araxes Paper Mill Aqueduct (APMA) over the river; c2) Panoramic view of the APMA; c3) Detail of the support of the APMA on the rock slope; d) Meteorological data for both sites (taken from Euskalmet, 2022).

Blanc (Damas Mollá et al., 2020), while José Eugenio Rivera, the engineer who designed the aqueduct, used his own patent to execute the structure (Ribera, 1925). These details are fundamentally important for understanding the way these structures were actually undertaken, i.e. the execution of construction, and their current state (Damas Mollá et al., 2020).

The horizontal structure of the Punta Begoña Galleries is made of ribbed slabs in reinforced concrete. In some areas, these are in the form of double slabs; one structural (upper) and the other, of lesser thickness (lower), which functions as a false ceiling. The slabs are supported by pillars, reinforced concrete columns and perforated brickwork. The aqueduct consists of an empty channel case, with two edge beams on the sides and an upper slab binding them together, and a lower slab suspended from them. This system is supported on 4 slender double palisades which transfer the loads through rectangular reinforced concrete supports resting on masonry piles [Construction Factor; Artistic Value: 0; Carving: 0; Finished: 0].

The morphology and architectural style also differ. The façades of the galleries are orientated perpendicularly to one another (allowing a comparison to be made between the two) [Construction Factor; Guidance: 2] and an eclectic style with exterior decorations [Construction Factor; Ornamentation: 1]. The aqueduct, on the other hand, is a linear structure [Construction Factor; Guidance: 0] with simple unornamented finishes [Construction Factor; Ornamentation: 0]. Importantly, neither of the constructions has undergone any significant alterations.

Another very significant difference is the use made of the two constructions. While the galleries were built for private, residential use [Construction Factor; Usage: 1], the aqueduct is a civil construction that forms part of an industrial complex [Construction Factor; Usage: 0]. Both have suffered several decades of neglect.

There are also a number of differences and similarities between the emplacements of the two constructions. Both structures are adapted to, or take advantage of, features in the existing relief and are supported directly on concrete pillars on the original solid rock — in the case of the galleries, a coastal cliff and in the case of the aqueduct, the solid rock of the bank of the Araxes River [Environmental Factor; Substrate: 0].

In terms of their environment, the galleries are situated in an urban, mainly recreational, environment, with some sources of industrial pollution (Madariaga et al., 2019) and clear influence from the coastal marine environment [Environmental Factor; Sea: 3], as they overlook the Ereaga beach. In contrast, the aqueduct stands in more rural surroundings and has clearly been affected by vegetation and the action of the river flowing under the structure. Both are in close proximity to road traffic — the galleries stand beside *Muelle de Ereaga* street, while the aqueduct runs over the GI-

ALTERATION	CONSTRUCTION	MATERIAL/ZONE AFFECTED	% ASA	DEGREE	ALTERATION INDEX	
A1b (Splitting)	APMA	Pillars	26%	●●●○○	AI	
		Slab	13%	●●○○○		
A1c (Craquele)	SWG	Columns in the upper terrace	2%	●○○○○	NWG	1
A1eI (Fracture with loss of stability)	NWG	Perimeter enclosure of the upper terrace	5%	●○○○○		
	SWG	Perimeter enclosure of the upper terrace	5%	●○○○○	SWG	1.8
		Façade, straight sections	25%	●●●○○		
		Union between façades	25%	●●●○○	APMA	2,5
A1eII (F. without loss of stability)	NWG	Column ending	0.1%	●○○○○		
	SWG	Column ending	0.1%	●○○○○		
B1a (Impact)	SWG	Columns	3%	●○○○○	BI	
B1e (Drilling)	NWG	Concrete quadrants	0	○○○○○		
	SWG	Concrete quadrants	0	○○○○○	NWG	1.14
B2 (Hiatus)	NWG	Vertical balustrade crosspieces	5%	●○○○○		
	SWG	Crosspieces of the corridor balustrade	5%	●○○○○		
B3 (Blistering)	SWG	Sandstone masonry and mortar rendering	30%	●●●○○		
B5c (Sanding)	NWG	Sandstone masonry	5%	●○○○○		
	SWG	Sandstone masonry	30%	●●●○○	SWG	1.55
B6 (Peeling)	NWG	Sandstone masonry	5%	●○○○○		
B7a (Flaking)	SWG	Sandstone masonry	15%	●●○○○		
B7b (Spalling)	NWG	Concrete quadrants	25%	●●●○○		
	SWG	Concrete quadrants	20%	●●○○○		
		Columns in the upper terrace	5%	●○○○○		
B7c (Contour flaking or spalling)	NWG	Horizontal crosspieces of the balustrade	5%	●○○○○	APMA	0
	SWG	Horizontal crosspieces of the balustrade	5%	●○○○○		
B9 (Alveolar weathering)	NWG	Sandstone masonry	5%	●○○○○		
	SWG	Sandstone masonry	18%	●●○○○		
		Horizontal crosspieces of the balustrade	2%	●○○○○		
C2 (Discolouration)	NWG	Southwest-facing façade	15%	●●○○○	CI	
C3 (Damp area)	NWG	Façade affected by broken gutters	30%	●●●○○		
	SWG	Façade affected by broken gutters	30%	●●●○○		
	APMA	Bottom part of slab (joint)	35%	●●●○○	NWG	2.5
		Support on rock	45%	●●●○○	SWG	3
C4 (Staining)	APMA	Lower slab	20%	●●○○○	APMA	2.67
D1a (Black Crust)	NWG	Balustrades and columns	7%	●○○○○	DI	
	SWG	Balustrades	5%	●○○○○		
D2b (Debris)	APMA	Inner case	17%	●●○○○		
	NWG	Entire facade in general	75%	●●●●○		
D2c (Soot)	SWG	Entire façade in general	60%	●●●●○	NWG	1.8
	APMA	Entire structure in general	18%	●●○○○		
D2e (Artificial)	APMA	Case side	1%	●○○○○		
D3 (Efflorescence)	NWG	Concrete quadrants	10%	●●○○○		
	SWG	Concrete quadrants	5%	●○○○○		
	APMA	Support on rock	9%	●○○○○	SWG	1.6
D4a/b (Encrustation)	NWG	Mortar	0.1%	●○○○○		
	SWG	Mortar	3%	●○○○○		
	APMA	Palisade (in curtain)	3%	●○○○○		
		Lower slab joint (encrustation)	9%	●○○○○	APMA	1.33
D5 (Graffiti)	NWG	Isolated on outer facade	5%	●○○○○		
	SWG	Isolated on outer façade	5%	●○○○○		
E1 (Algae)	APMA	Case	20%	●●○○○	EI	
		Foundation	22%	●●○○○		
E2 (Lichen)	NWG	Entire façade in general	75%	●●●●○		
	SWG	Entire façade in general	75%	●●●●○		
	APMA	Case	33%	●●●○○	NWG	2.5
E3 (Mould)	NWG	Masonry wall	25%	●●●○○		
	SWG	Masonry wall	25%	●●●○○		
	APMA	Case	30%	●●●○○		
E4(Moss)	APMA	Case	63%	●●●●○	SWG	2.4
E5 (Plants and larger organisms)	NWG	Masonry wall	12%	●○○○○		
		Concrete quadrant planters	30%	●●●○○		
		Perimeter vegetation at the base	20%	●●○○○		
		Upper terrace vegetation	20%	●●○○○		
	SWG	Masonry wall	12%	●○○○○		
		Perimeter vegetation at the base	30%	●●●○○	APMA	2.83
		Upper terrace vegetation	15%	●○○○○		
	APMA	Case	30%	●●●○○		

Fig. 4. Alterations in the Façades and Alteration indexes of the Punta Begoña galleries (NWG: Northwest Gallery; SWG: Southwest Gallery) and Araxes Paper Mill Aqueduct (APMA) according to the classification matrix by Damas Mollá et al. (2018) (ASA: Area of Structure Affected; AI, BI, CI; DI, EI AI, BI, CI, DI, EI: Alteration indexes, description in text).

Fig. 5. Main alterations in the façades of the Punta Begoña Galleries located on the point cloud of: a) NWG (Northwest Gallery); a1) A1eI: fracture without loss of stability, breakage, of the upper part of the column; a2) B6: peeling of masonry sandstones; a3) B7c: contour flaking of plastering mortar of balustrade crosspieces; a4) B7b: spalling of decorative plaster mortar of concrete quadrants of intermediate section; a5) E5: plants on roofing; a6) B2: hiatus in balustrade crosspieces; a7) D2c: soot on façade, columns (orange circles); a8) D1a: black crusts on sides of balustrade crosspieces in the gallery corridor; and b) Southwest Gallery (SWG); b1) B3: blistering in masonry wall sandstones; b2) B9: alveolar weathering in sandstones of masonry wall; b3) D4 a: calcium carbonate encrustations in curtain walls caused by degradation of the mortar used in the masonry; b4) C3: darkening from damp area on the curved façade of the SWG; b5) AleII: fracture with loss of stability (SWG); b6) A1c: cracking of plastering mortar of the intermediate concrete wall; b7) D3: white efflorescence on reinforced concrete of the intermediate quadrants; b8) E2/E3: bioalteration from lichen and mould. (Degree of effect: ○○○○○: no ASA; ●○○○○: <10 % ASA; ●●○○○: 10 % to 25 % of ASA; ●●●○○: 25 % to 50 % of ASA; ●●●●○: 50 % to 75 % of ASA; ●●●●●: all ASA) (based on Damas Mollá et al., 2018).

2135 main road, which supports heavy traffic [Environmental Factor; Pollution: 3]. More generally, both constructions are in an Atlantic climate zone and therefore have a broadly similar climate. A priori, however, the open location of the galleries overlooking the sea, as compared to the closed valley of the aqueduct might result in differences in terms of the effects of meteorological agents. Fig. 3d shows some meteorological information for both locations obtained from the Basque Meteorological Agency (Euskalmet) (Euskalmet, 2022).

4. Results: application of methodology

The process used for obtaining the AFV diagrams for each of the façades of the Punta Begoña Galleries (NWG and SWG) and for the Araxes Paper Mill Aqueduct (APMA) is set out below.

The first step involves characterising the alterations (A) in the two constructions. Fig. 4 shows the data obtained and specifies the location and area of the structure where each of the alterations was recorded, as

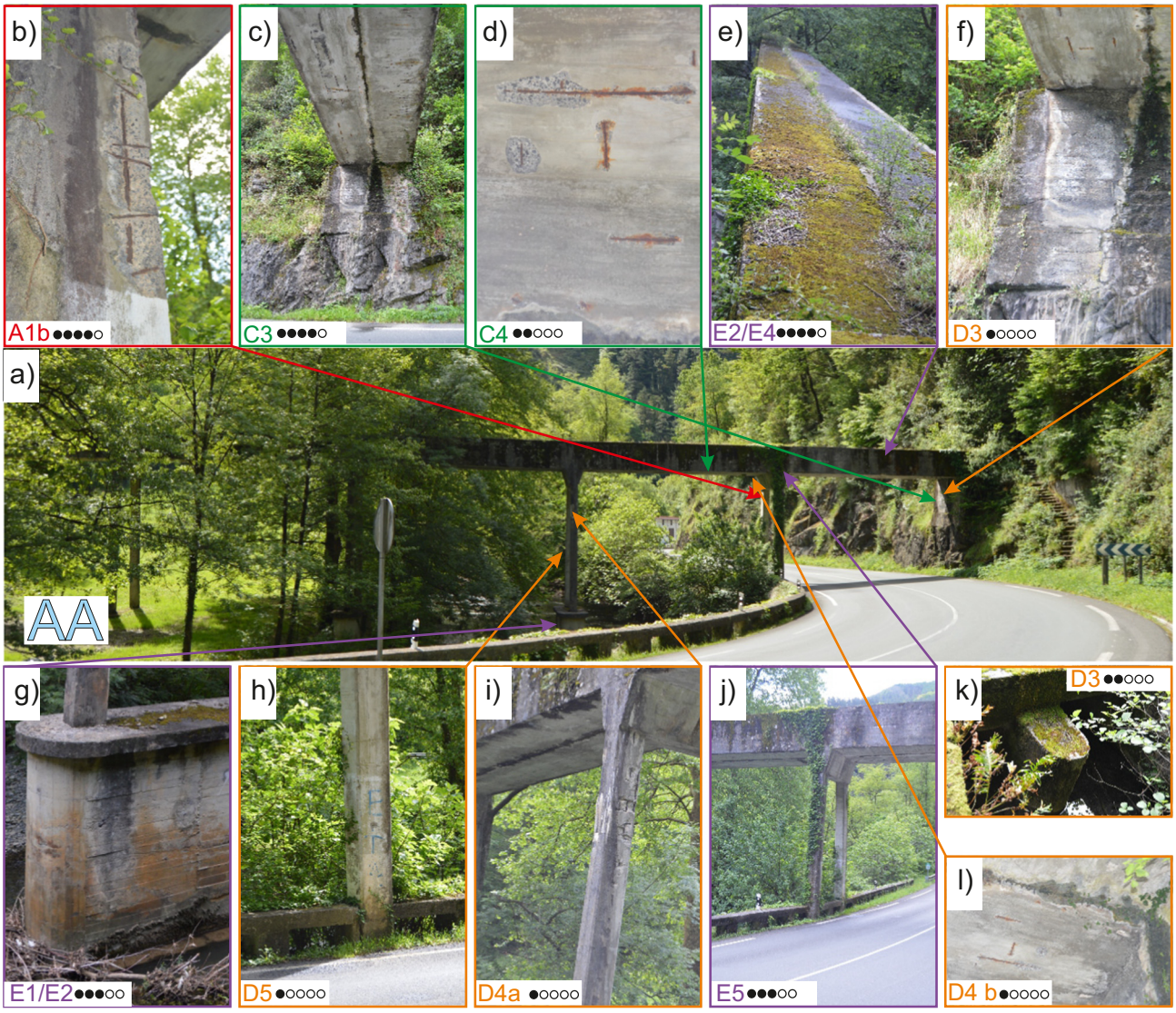

Fig. 6. Main alterations in the Araxes Paper Mil Aqueduct (APMA): a) Side view of the aqueduct; b) A1b: splitting; c) C3: darkening from damp zone in the support with the rock; d) C4: Staining of concrete due to degradation of metal reinforcement at the base of the case; e) E2 and E4: lichen and moss on the case; f) D3: efflorescence in the area of support with the rock; g) E1 and E2: algae and lichen at the base of the palisades above the river; h) D5: graffiti on pillar; i) D4a: encrustation in curtain on palisade; j) E5: creeper-type plant on palisade; k) D2b: debris inside case; l) D4b: macaroni-type encrustations in the bottom joint of the case (Degree of effect: ○○○○○: no ASA; ●○○○○: <10 % ASA; ●●○○○: 10 % to 25 % of ASA; ●●●○○: 25 % to 50 % of ASA; ●●●●○: 50 % to 75 % of ASA; ●●●●●: all ASA) (based on Damas Mollá et al., 2018).

well as the percentage of the Area of the Structure Affected by this alteration (ASA), and the degree thus calculated. A significant number of varying alterations were recorded in both constructions. Some examples of the most representative ones are shown in Figs. 5 and 6. Using the data on degree and by quantifying the number of alterations of each main type, the alteration indexes (AI, BI, CI, DI and EI) are calculated, based on Formula (1). The calculation of the three A-type alteration indexes (AI) is presented below as an example. In the APMA, 2 records of type A alterations have been recorded, in the pillars and in the slab. According to the relationship established between the percentages of ASA and the degree, a total of 5 scores (3 in the pillars and 2 in the slab) were recorded. The AI of the ASA established is 2.5 and is calculated by dividing the total number of scores by the number of records of alterations of this type, therefore, 5 by 2. In the case of the SWG, a total of 5 records have been recorded, in the columns of the upper terrace; in the perimeter enclosure of the upper terrace; in the façade, straight sections; in the union between the façades; and, in the column terminations. In this case the total number of degree scores is 9 (two records have a degree of 3 and three records have a degree of 1). Therefore, the IA of the SWG is 1.8. The NWG records 2 records in total, in the perimeter enclosure of the upper terrace and column ending. The sum of scores is 2, one for each record. Therefore the AI in this case is 1. The results obtained (Fig. 4) are projected on each of the radii of the pentagons in the AFV diagram (Fig. 7).

The following vulnerability matrix shows the data obtained after weighting the different factors (F) using the cases proposed in Table I in the case of the two façades of the Galleries (NWG and SWG) and in the case of the APMA. Using these data, the Vulnerability Indices were calculated based on the Factors ($F_{C,M\ or\ N}VI$) and the Global Vulnerability Index ($V_G I$) (Fig. 2). The results obtained were projected onto the corresponding blocks of the AFM diagram (Fig. 7). In the case of the façades of the galleries, by superimposing the results, it is also possible to make direct comparisons between the two areas of the construction (Fig. 7).

The AFV diagram (Fig. 7) allows relationships to be established between the different indexes, based on the vulnerability of the construction and/or each part of the construction. In the case of the Punta Begoña Galleries, the alteration pentagon shows a larger shaded area in the SWG than in the NWG; the overall degree of alteration of the SWG is slightly higher. Even so, the alteration indexes obtained for both façades fell within the

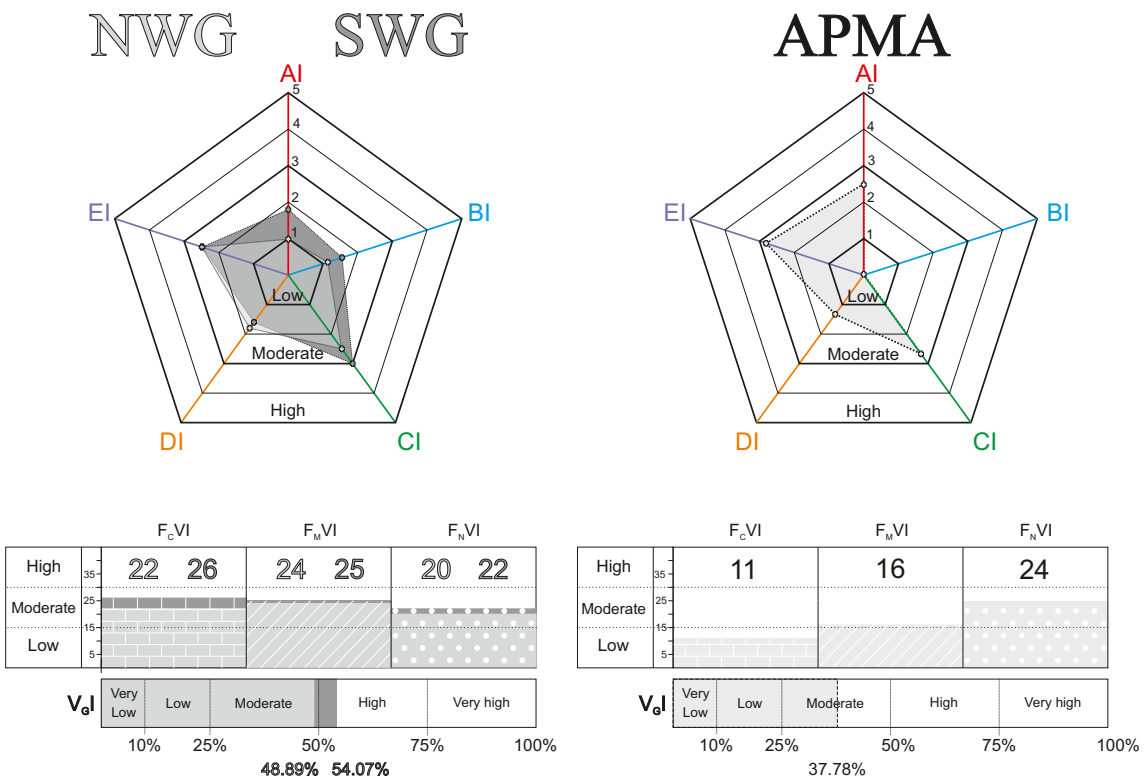

Fig. 7. AFV diagram obtained in the two construction analysed. Punta Begoña Galleries (NWG: Northwest Gallery; SWG: Southwest Gallery) and Araxes Paper Mill Aqueduct (APMA). (AI, BI, CI, DI, EI: Alteration Indexes; F_CVI: Vulnerability index according to Construction Factors; F_MVI: Vulnerability Index according to factors intrinsic to the materials; F_NVI: Vulnerability Index according to Natural Factors; V_GI: Global Vulnerability Index).

'moderate alteration' range. In both cases, the types of alteration showing most effect are those of Category C (chromatic alteration) and E (bioalterations). The indexes of type A (crack) and type B (mechanical damage and detachment) alterations are also slightly higher in SWG. The blocks of indices of factors affecting vulnerability (FVI) also fall within the moderate range; the greatest difference is found in the values obtained in the F_CVI (22 for the NWG and 26 for the SWG). The other two indexes show similar values but are slightly higher for SWG (24 and 25 for F_MVI) (20 and 22 for F_NVI). The V_GI of the NWG (48.89 %) stands within the moderate range, like the other partial indexes associated with the factors. However, when taking into account the factor indexes of the SWG as a whole, the V_GI is higher, standing within the 'high' range (54.07 %).

The APMA has a different distribution of alteration indexes to the Punta Begoña Galleries (Fig. 7). Although also within the moderate range, they are somewhat higher, verging on the 'high' range, especially those of alteration category A (cracks), which has a value of 2.5. It is also worth noting the lack of type B alterations (mechanical damages and detachment). As in the case of the galleries, the blocks representing the vulnerability indices with regard to the main factors (FVI), stand within the moderate range, but with lower values in the first two (11 for F_CVI and 16 for F_MVI) and somewhat higher in that obtained for F_NVI (24). The value obtained for the Global Vulnerability index of the APMA is moderate (37.78 %), also lower than those of the façades of the Punta Begoña Galleries.

5. Discussion

The following are some of the main aspects of the data obtained for the Punta Begoña Galleries:

Type A (crack) alterations have developed mainly in the SWG (Fig. 5 b5). Consequently, the highest values of F_CVI were also obtained in this area.

Type B alterations, such as detachments, are caused by an interaction between factors intrinsic to the materials and natural factors, especially weather impacts. In this regard, the texture, composition and compatibility of the different materials of the galleries influences the degree of weathering they suffer. The main alterations of this type recorded are of type B5 (disintegration) in the sandstones of the masonry section (Fig. 5 b1), and of type B7b (spalling) (Fig. 5 a4), in the concrete quadrants, where the covering mortar is spalled. The materials used in the two façades are similar and for this reason, the values obtained for F_MVI in NWG and SWG are also similar. The F_NVI is also similar in the two study areas, mainly due to the climate of the area in which the galleries are located: a mesothermal Atlantic climate, with mild temperatures and very high rainfall (Euskalmet, 2022). However, the index is higher in SWG. This is due to the orientation of the façade itself leading to greater intensity of some weather impact factors, aerosols, pollutants (Madariaga et al., 2019) and exposure to sunlight.

For type C alterations (Chromatic), the CI of SWG is higher than that of NWG. In the galleries, this type of alteration is caused by breakage and lack of maintenance. In the case of NWG, clogged and/or broken guttering systems were recorded throughout the façade. In addition, due to its orientation, this façade receives fewer hours of direct sunlight, so damp areas remain damp over time. In SWG, the Type C3 alteration (darkening due to damp areas) (Fig. 5 b4), is largely concentrated in the curved portion of the façade. The main factors involved are the morphology of this part of the façade, the hours of sunlight (F_NVI) and, above all, the condition of maintenance of the roof (F_CVI).

The DIs of both façades are in the medium range and are similar for the two façades; type D alterations are mainly deposits of exogenous materials, primarily soot (Fig. 5 a7), accumulated as a result of the proximity of road traffic. In some specific areas, there is also some shrinkage due to degradation of the rendering mortar of the masonry wall (Fig. 5 b3) or the concrete of the structure itself. These types of alterations are therefore related to the three main types of factors analysed, especially the last two (F_MVI and F_NVI). The same is true of EI; the range obtained is somewhat higher in NWG because of the vegetation on the roof (Fig. 5 a5). This type of

alteration is also the result of lack of maintenance and the climate of the environment.

In the case of the results obtained for the Araxes Paper Mill Aqueduct (APMA) the chief aspects are as follows:

The highest value is for AI alteration index (type A, cracks). These alterations are of splitting type (A1b), caused by degradation of the concrete reinforcement and loss of its covering (Fig. 6b). An analysis of the FVI results indicates that this corrosion is not only due to construction factors or the construction material itself, since both the F_CVI and the F_MVI stand within the moderate range. This alteration has been generated by a conjunction of both, which is also intensified by the natural conditions to which the structure is subjected (F_NVI moderate).

Bioalterations (type E alterations) are the second highest type of index and stand in the medium range. This type of alteration is caused by the rural environment in which it is located (F_NVI) and lack of maintenance of the structure (F_CVI). All kinds of bioalteration, algae and lichens have been recorded, mainly at the base of the pillars (Fig. 6g) and moss, mould and plants at the top of the case (Fig. 6e).

Alterations of type C (Chromatic Changes) are not very significant in this construction. In general, they may be related to others of greater incidence such as the orange staining (C3) related to degradation of the reinforcements (Fig. 6d). In some areas there is also darkening due to constant damp (C3) (Fig. 6f). This is to be expected, given that the construction under study is an aqueduct and is mainly the result of lack of maintenance.

The type D alterations (deposits) are basically deposits of exogenous materials, mainly of soot type, on the surface, as a result of the heavy road traffic under this structure. This type of alteration shows the relationship between natural and environmental factors and vulnerability. In this case the F_NVI is the highest. Numerous calcium carbonate encrustations have also formed, (Fig. 6f, i); the factors intrinsic to the materials and construction factors are mainly responsible for their formation, since they are recorded in the area of the joins between slabs, but the humid environment typical of the surrounding Atlantic climate also plays a role. Proper maintenance of the structure would contribute to reducing many of these alteration indexes. Regarding the value obtained for F_CVI, the generally good state of the structure is noteworthy, bearing in mind its age and the lack of regulatory standards on concrete construction at the beginning of the century. The low F_MVI result is also notable, but this is due to the use of a single construction material and the simplicity of the structure itself, with straight lines, in contrast to the Punta Begoña Galleries.

6. Conclusions

The use of the AFV diagrams in context, both with the construction and with its emplacement and environment, allows a precise assessment of Global Vulnerability in Cultural Built Heritage.

The methodology designed has been applied to two early twentieth-century reinforced concrete heritage buildings in the Basque Country: the Punta Begoña Galleries (Getxo), where two façades with perpendicular orientations (NWG and SWG) were analysed, and a work of civil engineering, the Aqueduct of the Araxes Paper Mill (APMA) (Tolosa). In summary, in each of the constructions, we established: 1) the type of predominant alterations with the alteration indexes; 2) the factors involved in its deterioration; and 3) its vulnerability. All this information has been synthesised in the AFV diagrams for each construction, which could then be compared, taking the specific context of each one into account.

In this study, we have chosen to concentrate on heritage elements in reinforced concrete, since this type of constructions presents an additional vulnerability, namely a lack of social and cultural awareness of the importance of these assets (ICOMOS, 2014). A comprehensive diagnosis of construction methods and state of preservation is indispensable for revitalising historic concrete buildings (Custance-Baker and Macdonald, 2014; Heinemann, 2008; Heinemann, 2013; Heinemann et al., 2010; ICOMOS, 2014). Nonetheless, the methodology presented here could also be used in constructions made from other materials.

As regards the study of alterations, we have used the alteration characterisation matrix of Damas Mollá et al., 2018 which is based on ICOMOS (2010). On this occasion, these alterations have been further quantified using the alteration indices with respect to the percentage of the area of the structure affected.

In establishing the factors involved in the vulnerability of constructions, which are responsible for alterations, it is essential to extend the study to both the emplacement and the environment; a construction should not be analysed in isolation. In this regard, the data obtained in the AFV diagrams of the Punta Begoña Galleries and the Aqueduct of the Araxes Paper Mill show that there is no single factor involved. All the factors implicated in vulnerability (including construction factors, factors intrinsic to the materials, natural factors and environmental factors) interact with one another. One of the key points of the proposed methodology, therefore, is this possibility of directly relating the main types of alteration with the factors involved in the vulnerability of each area or construction under study.

The indexes established for each parameter of the AFV diagram allow it to be quantified and represented in graph form, facilitating interpretation of the results. In this case, by selecting construction elements with differences it has been possible to demonstrate that the use of the same scales allows analogous comparisons to be made, not only between different construction elements (application of the methodology was validated in a residential building and in a civil engineering structure), but also between different areas of the same construction.

The methodology presented is systematic and, most importantly, replicable in different contexts. Moreover, it allows direct comparisons to be made between different areas of the same construction and between different constructions, through superimposition of the AFV diagrams. The vulnerability analysis, based on the main factors presented, and the parallel characterisation and quantification of the alterations found, offers key information for an initial approximation of the real state of a construction or study area. Using this information, it is possible to plan and prioritise the actions required to mitigate this vulnerability. In addition, by establishing which factors have the greatest impact on this vulnerability, other more detailed specific studies can be launched.

CRediT authorship contribution statement

Damas Mollá Laura: Ideas; formulation or evolution of the overall research objectives and goals. Development or design of methodology. Data collection. Validation. Preparation of text and figures.

Sagarna Maialen: Development or design of methodology. Data collection. Validation. Preparation of text and figures.

Zabaleta Ane: Development or design of methodology. Preparation of text and figures.

Aranburu Arantza: Development or design of methodology. Validation. Preparation of text and figures.

Antiguedad Iñaki: Supervisory and leadership responsibility for the planning and execution of the research activity. Acquisition of financial support for the project leading to this publication.

Uriarte Jesus A: Ideas; formulation or evolution of the overall research objectives and goals. Development or design of the methodology. Preparation of text and figures. Management responsibility and coordination of the planning and execution of the research activity.

Declaration of competing interest

The authors declare that they have no known competing financial interests or personal relationships that could have appeared to influence the work reported in this paper.

Acknowledgments

This study was conducted by UPV/EHU Research Group IT-1029/16 (Government of the Basque Country) in the framework of the project titled "*Puesta en valor del inmueble histórico cultural Galerías Punta Begoña (Getxo,*

Bizkaia)" ["Revitalising the Punta Begoña Galleries, a culturally historic building in Getxo, Biscay Province"], under a cooperation agreement between the University of the Basque Country (UPV/EHU) and the City Council of Getxo (OTRI2019-0318). The authors are very grateful for the comments and suggestions of the referees, which have undoubtedly improved the original manuscript.

References

Alonso, F.J., Esbert, R.M., Ordaz, J., Vázquez, P., 2006. Análisis del deterioro en los materiales pétreos de edificación. ReCoPaR 3, 23–32.

Alonso, F.J., Ordaz, J., Grossi, C., Díaz-Pache, F., Esbert, R.M., 1998. Características petrográficas que condicionan la durabilidad de la piedra natural. Actas 2nd Congr. Int. Piedra, Madrid.

Álvarez, I., Bodego, A., Aranburu, A., Arriolabengoa, M., del Val, M., Iriarte, E., Abendaño, V., Calvo, J.I., Garate Maidagan, D., Hermoso de Mendoza, A., Ibarra, F., Legarrea, J., Tapia Sagarna, J., Agirre Mauleon, J., 2017. Geological risk assessment for rock art protection in karstic caves (Alkerdi Caves, Navarre, Spain). J. Cult. Herit. 33, 170–180. https://doi.org/10.1016/j.culher.2018.01.017.

ASM International, 2002. Thermal Properties of Metals. ASM International, Ohio.

Bera, S., Guru, B., Oommen, T., 2020. Indicator-based approach for assigning physical vulnerability of the houses to landslide hazard in the Himalayan region of India. Int. J. Disaster Risk Reduct. 50, e101891. https://doi.org/10.1016/j.ijdrr.2020.101891.

Bienvenido-Huertas, D., León-Muñoz, M., Martín-del-Río, J.J., Rubio-Bellido, C., 2021. Analysis of climate change impact on the preservation of heritage elements in historic buildings with a deficient indoor microclimate in warm regions. Build. Environ. 200, 107959. https://doi.org/10.1016/j.buildenv.2021.107959.

Bonazza, A., Sardella, A., Kaiser, A., Cacciotti, R., De Nuntiis, P., Hanus, C., Maxwell, I., Drdácký, T., Drdácký, M., 2021. Safeguarding cultural heritage from climate change related hydrometeorological hazards in Central Europe. Int. J. Disaster Risk Reduct. 63, 102455. https://doi.org/10.1016/j.ijdrr.2021.102455.

Borri, A., Corradi, M., De Maria, A., 2020. The failure of masonry walls by disaggregation and the Masonry Quality Index. Heritage 3, 1162–1198. https://doi.org/10.3390/heritage3040065.

Broto, C., 2006. Enciclopedia Broto de las patologías de la construcción. Links International, Barcelona.

Cacciotti, R., Kaiser, A., Sardella, A., De Nuntiis, P., Drdácký, M., Hanus, C., Bonazza, A., 2021. Climate change-induced disasters and cultural heritage: optimizing management strategies in Central Europe. Clim. Risk Manag. 32, 100301. https://doi.org/10.1016/j.crm.2021.100301.

Colegio de Ingenieros de Caminos, Canales y.Puertos de Madridcollab, 1982. José Eugenio Ribera Dutasta, Ingeniero de Caminos (1864-1936). Colegio de Ingenieros de Caminos, Canales y Puertos, Madrid.

CTE, 2022. Código Técnico de la Edificación. https://www.codigotecnico.org/. (Accessed 6 June 2022).

Custance-Baker, A., Macdonald, S.T., 2014. Conserving Concrete Heritage Experts Meeting. The Getty Conservation Institute, Los Angeles.

Daly, C., 2014. A framework for assessing the vulnerability of archaeological sites to climate change: theory, development, and application. Conserv. Manag. Archaeol. Sites 16, 268–282. https://doi.org/10.1179/1350503315Z.00000000086.

Damas Mollá, L., Uriarte, J.A., Aranburu, A., Bodego, A., Balciscueta, U., García Garmilla, F., Morales, T., 2018. Systematic alteration survey and stone provenance for restoring heritage buildings: Punta Begoña Galleries (Basque-Country, Spain). Eng. Geol. 247, 12–26. https://doi.org/10.1016/j.enggeo.2018.10.009.

Damas Mollá, L., Zabaleta, A., Uriarte, J.A., Aranburu, A., Sagarna, M., Morales, T., 2019. Geology and built cultural heritage: the transdisciplinary approach in the Punta Begona Galleries (Getxo, Bizkaia). Geogaceta 66, 123–126.

Damas Mollá, L., Sagarna Aranburu, M., Uriarte, J.A., Aranburu, A., Zabaleta, A., García-García, F., Antigüedad, I., Morales, T., 2020. Understanding the pioneering techniques in reinforced concrete: the case of Punta Begoña Galleries, Getxo,Spain. Buil. Res. Inf. 48, 785–801. https://doi.org/10.1080/09613218.2019.1702498.

Day, J.C., Heron, S.F., Markham, A., 2020. Assessing the climate vulnerability of the world's natural and cultural heritage. Parks Stewardsh. Forum 36, 144–153. https://doi.org/10.5070/P536146384.

D'Ayala, D., Yuan Yan, K.W., Smith, H., Massam, A., Filipova, F., Pereira, J.J., 2020. Flood vulnerability and risk assessment of urban traditional buildings in a heritage district of Kuala Lumpur,Malaysia. Nat. Hazards Earth Syst. Sci. 20, 2221–2241. https://doi.org/10.5194/nhess-20-2221-2020.

Edmonds, H.K., Lovell, J.E., Lovell, C.A.K., 2020. A new composite climate change vulnerability index. Ecol. Indic. 117, 106529. https://doi.org/10.1016/j.ecolind.2020.106529.

Esbert, R.M., Ordaz, J., Alonso, F.J., Montoto, M., González Limon, T., Álvarez de Buergo, M., 1997. Manual de diagnosis y tratamiento de materiales pétreos y cerámicos. Colegio de aparejadores y Arquitectos técnicos de Barcelona, Barcelona.

European Center for Geodynamics and Seismology, 1998. European Macroseismic Scale 1998. vol. 15. Cahiers du Centre Européen de Géodynamique et de Séismologie.

Euskalmet, 2022. Agencia Vasca de Meteorología (Basque Meteorological Agency). https://euskalmet.beta.euskadi.eus/s07-5853x/es/meteorologia/home.apl?e=5. (Accessed 3 February 2022).

Fais, S., Casula, G., Cuccuru, F., Ligas, P., Bianchi, M.G., 2018. An innovative methodology for the non-destructive diagnosis of architectural elements of ancient historical buildings. Sci. Rep. 8, e4334. https://doi.org/10.1038/s41598-018-22601-5.

Fakhruddin, B.(.S.H.M)., Reinen-Hamill, R., Robertson, R., 2019. Extent and evaluation of vulnerability for disaster risk reduction of urban Nuku'alofa. Tonga. Prog. Disaster Sci. 2, e100017. https://doi.org/10.1016/j.pdisas.2019.100017.

Fatorić, S., Biesbroek, R., 2020. Adapting cultural heritage to climate change impacts in the Netherlands: barriers, interdependencies, and strategies for overcoming them. Clim. Chang. 162, 301–320. https://doi.org/10.1007/s10584-020-02831-1.

Formisano, A., Marzo, A., 2017. Simplified and refined methods for seismic vulnerability assessment and retrofitting of an Italian cultural heritage masonry building. Comput. Struct. 180, 13–26. https://doi.org/10.1016/j.compstruc.2016.07.005.

Fotopoulou, S.D., Pitilakis, K.D., 2017. Vulnerability assessment of reinforced concrete buildings at precarious slopes subjected to combined ground shaking and earthquake induced landslide. Soil Dyn. Earthq. Eng. 93, 84–98. https://doi.org/10.1016/j.soildyn.2016.12.007.

Galan, E., Aparicio, P., 2013. The environmental risk assessment applied to cultural heritage. A methodological approach. In: Boriani, M., Gabaglio, R., Gulotta, D. (Eds.), Proc. Conf. Built Herit. 2013 Monitor. Conserv. Manag. Centro per la Conservazione e Valorizzazione del Beni Culturali, Milan, pp. 1405–1409.

Gandini, A., Egusquiza, A., Garmendia, L., San José, J.T., 2018. Vulnerability assessment of cultural heritage sites towards flooding events. IOP Conf. Ser.: Mater. Sci. Eng. 364, e012028. https://doi.org/10.1088/1757-899X/364/1/012028.

Gobierno Vasco, 2001. Patrimonio del País Vasco (Basque Country Heritage). https://www.euskadi.eus/app/ondarea/patrimonio-construido/galerias-de-punta-begona/galeria-pasadizo/getxo-bizkaia-/fichaconsulta/29755/. (Accessed 3 February 2022).

Gobierno Vasco, 2017. Boletín Oficial del Gobierno Vasco (Official Bulletin of the Basque Government). http://www.euskadi.eus/bopv2/datos/2017/07/1703795a.pdf. (Accessed 3 February 2022).

Hatir, M.E., 2020. Determining the weathering classification of stone cultural heritage via the analytic hierarchy process and fuzzy logic inference system. J. Cult. Herit. 44, 120–134. https://doi.org/10.1016/j.culher.2020.02.011.

Heinemann, H.A., 2008. Why historic concrete buildings need holistic surveys. In: Walraven, J.C., Stoelhorst, D. (Eds.), Proc. Int. FIB Symp. 2008 - Tailor Made Concrete Structures - New Solutions for our Society. FIB Int. Fed. Struct. Concrete, Amsterdam, pp. 103–108.

Heinemann, H.A., 2013. Forgotten material history of historic concrete. Proc. IABSE Conference: Assessment, Upgrading And Refurbishment of Infrastructures. Int. Assoc. Bridge Struct. Eng., Rotterdam, pp. 358–359.

Heinemann, H.A., Zijlstra, H., Nijland, T.G., Van Hess, R.P.J., 2010. The challenge of a perpetual service life: the conservation of concrete heritage. In: van Breugel, K., Ye, G., Yuan, Y. (Eds.), Proc. 2nd Int. Symp. Serv. Life Design Infrastruct. RILEM Publications, Delf, pp. 1067–1074.

IGN, 2022. Instituto Geográfico Nacional (National Geographical Institute). https://www.ign.es/web/ign/portal/. (Accessed 6 June 2022).

ICOMOS (International Council on Monuments and Sites), 2010. Illustrated Glossary on Stone Deterioration Patterns. ICOMOS International Scientific Committee for Stone, Paris.

ICOMOS (International Council on Monuments and Sites), 2014. Approaches for the Conservation of Twentieth Century Architectural Heritage. ICOMOS International Scientific Committee on 20th Century Heritage, Madrid.

Laborde Marqueze, A., 2013. COREMANS Project: "Criteria for Working in Stone Materials". Ministerio de Educación, Cultura y Deporte, Madrid.

Macías-Bernal, J.M., Calama-Rodríguez, J.M., Chávez-de Diego, M.J., 2014. Prediction model of the useful life of a heritage building from fuzzy logic. Inf. Constr. 66, e006. https://doi.org/10.3989/ic.12.107.

Madariaga, I., Lama, E., Calparsoro, E., Prieto-Taboada, N., Arana, G., Rodríguez Laso, M.D., Madariaga, J.M., 2019. Enhancement and recovery of the tiles affected by atmospheric pollutants in the Galleries of Punta Begoña, Getxo (Bizkaia). Bol. Soc. Esp. Ceram. 58, 161–170. https://doi.org/10.1016/j.bsecv.2018.11.001.

Mateos Redondo, F., 2012. Aportación de la Geología a la conservación del patrimonio histórico-artístico. In: Berrezuela Alvarado, E., Domínguez-Cuesta, M.J. (Eds.), Técnicas aplicadas a la caracterización y aprovechamiento de Recursos Geológico-Mineros. Volumen III: interacción con la sociedad. IGME, Oviedo, pp. 150–161.

Mattei, G., Rizzo, A., Anfuso, G., Aucelli, P.P.C., Gracia, F.J., 2019. A tool for evaluating the archaeological heritage vulnerability to coastal processes: the case study of Naples Gulf (southern Italy). Ocean Coast. Manag. 179, e104876. https://doi.org/10.1016/j.ocecoaman.2019.104876.

Moropoulou, A., Labropoulos, K.C., Delegou, E.T., Karoglou, M., Bakolas, A., 2013. Non-destructive techniques as a tool for the protection of built cultural heritage. Constr. Build. Mater. 48, 1222–1239. https://doi.org/10.1016/j.conbuildmat.2013.03.044.

Ortiz, R., Ortiz, P., 2016a. Vulnerability index: a new approach for preventive conservation of monuments. Int. J. Archit. Herit. 10, 1078–1100. https://doi.org/10.1080/15583058.2016.1186758.

Ortiz, R., Ortiz, P., 2016b. How to evaluate and mitigate vulnerability of historical buildings. A Spanish project experience. Energ. Ambiente Innov. 4, 89–93. https://doi.org/10.12910/EAI2016-064.

Papathoma-Köhle, M., Gems, B., Sturm, M., Fuchs, S., 2017. Matrices, curves and indicators: a review of approaches to assess physical vulnerability to debris flows. Earth-Sci. Rev. 171, 272–288. https://doi.org/10.1016/j.earscirev.2017.06.007.

Pope, G.A., Meierding, T.C., Paradise, T.R., 2002. Geomorphology's role in the study of weathering of cultural stone. Geomorphology 47, 211–225. https://doi.org/10.1016/S0169-555X(02)00098-3.

Prasetyo, Y.T., Senoro, D.B., German, J.D., Aurelius, R., Robielos, C., Ney, F.P., 2020. Confirmatory factor analysis of vulnerability to natural hazards: a household Vulnerability Assessment in Marinduque Island,Philippines. Int. J. Disaster Risk Reduct. 50, e101831. https://doi.org/10.1016/j.ijdrr.2020.101831.

Prieto, A.J., Verichev, K., Carpio, M., 2020. Heritage, resilience and climate change: a fuzzy logic application in timber-framed masonry buildings in Valparaíso,Chile. Build. Environ. 174, e106657. https://doi.org/10.1016/j.buildenv.2020.106657.

Quagliarini, E., Lucesoli, M., Bernardini, G., 2019. Rapid tools for assessing building heritage's seismic vulnerability: a preliminary reliability analysis. J. Cult. Herit. 39, 130–139. https://doi.org/10.1016/j.culher.2019.03.008.

Reeder-Myers, L.A., 2015. Cultural heritage at risk in the twenty-first century: a vulnerability assessment of coastal archaeological sites in the United States. J. Isl. Coast. Archaeol. 10, 436–445. https://doi.org/10.1080/15564894.2015.1008074.

Ribera, J.E., 1902. Hormigón y cemento armado. Mi sistema y mis obras, Ricardo Rojas, Madrid.

Ribera, J.E., 1925. Puentes de fábrica y hormigón armado. Tomo I, Generalidades, muros y pequeñas obras. Talleres Gráficos Herrera, Madrid.

Rodríguez-Rosales, B., Abreu, D., Ortiz, R., Becerra, J., Cepero-Acán, A.E., Vázquez, M.A., Ortiz, P., 2021. Risk and vulnerability assessment in coastal environments applied to heritage buildings in Havana (Cuba) and Cadiz (Spain). Sci. Total Environ. 750, e141617. https://doi.org/10.1016/j.scitotenv.2020.141617.

Sagarna, M., 2010. Gipuzkoako arkitekturaren eboluzioaren azterketa hormigoi armatuaren garapenari lotuta - Study of the Evolution of the Architecture of Gipuzkoa Linked to the Development of Reinforced Concrete. University of the Basque Country, Donostia-San Sebastián (Unpublished doctoral dissertation).

Sánchez-Delgado, N., Calleja, L., Rodrígez-Rey, A., Setien, A., De Argandoña, V.G., 2016. Critical review of abrasivity tests in rocks and the influence of the petrographic features. Trabajos de Geología. 36. Universidad de Oviedo, pp. 347–366.

Sesana, E., Gagnon, A.S., Bertolin, C., Hughes, J., 2018. Adapting cultural heritage to climate change risks: perspectives of cultural heritage experts in Europe. Geosciences 8, 305. https://doi.org/10.3390/geosciences8080305.

URA, 2022. Agencia Vasca del Agua (Basque Water Agency). https://www.uragentzia.euskadi.eus/inicio/. (Accessed 6 June 2022).

Valuzzi, M.R., Calò, S., Giacometti, G., 2020. Correlation of vulnerability and damage between artistic assets and structural elements: the DataBAES archive for the conservation planning of CH masonry buildings in seismic areas. Sustainability 12, 653. https://doi.org/10.3390/su12020653.